Modified Sedimentation-Dispersion Model for Solids in a Three-Phase Slurry Column

Solids distribution data for a three-phase, batch-fluidized slurry bubble column (SBC) are presented, using air as the gas phase, pure liquids and solutions as the liquid phase, and glass beads and carborundum catalyst powder as the solid phase. Solids distribution data for the three-phase SBC operated in a continuous mode of operation are also presented, using nitrogen as the gas phase, water as the liquid phase, and glass beads as the solid phase. A new model to provide a reasonable approach to predict solids concentration distributions for systems containing polydispersed solids is presented. The model is a modification of standard sedimentation-dispersion model published earlier. Empirical correlations for prediction of hindered settling velocity and solids dispersion coefficient for systems containing polydispersed solids are presented.

A new method of evaluating critical gas velocity (CGV) from concentrations of the sample withdrawn at the same port of the SBC is presented. Also presented is a new mapping for CGV which separates the two regimes in the SBC, namely, incomplete fluidization and complete fluidization.

D.N. Smith and J.A. Ruether
Pittsburgh Energy Technology Center
U.S. Department of Energy
Pittsburgh, PA 15236

Y.T. Shah and M.N. Badgujar
Department of Chemical/
Petroleum Engineering
University of Pittsburgh
Pittsburgh, PA 15261

SCOPE

Formulation of a mathematical model describing the behavior of solid particles in a slurry bubble column reactor usually includes the transport mechanisms of solids dispersion and hindered settling. In general, material balances for the axial variation of solids concentration is considered in model formulations. Unfortunately, the boundary conditions associated with analytical expressions describing axial solids concentration distributions are very difficult to obtain, either experimentally or theoretically. Moreover, in most instances slurry bubble column reactors contain solids having a particle size distribution that may not be uniformly dispersed throughout the reactor. For these reasons, the development of a mathematical model that has a closed form solution and considers the effect of particle size distribution would be desirable for improved understanding of solids behavior in a slurry bubble column reactor.

This study aims to investigate solids behavior in a slurry bubble column with monodispersed and polydispersed particle systems. A strategy is developed to analyze axial solids concentration distribution of polydispersed particles and boundary conditions are formulated that provide for a closed form solution of the sedimentation-dispersion model. The velocity required to completely suspend the particles (critical gas velocity) is implicitly obtained from the present model. Thus the model is useful for determining the range of operating conditions where completely suspended particles exist, and further addresses the hydrodynamic and mass transfer properties of slurry reactors containing polydispersed solids.

CONCLUSIONS AND SIGNIFICANCE

A modified sedimentation-dispersion model has been developed describing axial solids concentration distributions in a slurry bubble column. The model has been used mainly to study the effect of polydispersed solids on axial solids concentration and particle size distributions. In addition, a criterion for complete sus-

pension of the particles is developed from the present model, which is limited by the void fraction of solids at minimum fluidization conditions. According to model assumptions, the interaction of large and small particles is considered to have a negligible effect on hindered settling velocities and solid mixing of the respective particle sizes. Through analysis of experimentally obtained axial solids concentration distributions of binary and ternary particle size mixtures, this assumption is shown to be reasonably valid.

The results have revealed that changes in gas velocity have a small effect on the axial solids concentration distribution of completely suspended particles. In a similar manner, slurry velocity has only a slightly greater influence on solids distributions.

As expected, polydispersed particles have a greater variance in axial solids concentration distribution than do monodispersed particles having the same mean particle diameter. The axial particle size distribution for polydispersed particles indicates that significant segregation occurs for particle size ratios greater than two. It was expected that the axial variation in particle size might create a more uniform specific interfacial area of solids for the polydispersed particles as compared to the monodispersed particles. However, the monodispersed solids were found to have a more uniform and larger specific interfacial area than polydispersed particles for a given mean particle diameter. This is a result of the larger variance in axial solids concentration distribution for the polydispersed particles.

Introduction

Three-phase slurry bubble column (SBC) reactors are widely used in the hydroprocessing and fermentation industries and have been the subject of active research for more than two decades. SBC reactors have recently been used in direct coal liquefaction and for Fischer-Tropsch reaction, and they are finding increasing use in numerous other petrochemical industries (L'Homme, 1979; Chaudhari and Ramachandran, 1980; Brian and Dyer, 1984). The SBC can be operated in a semibatch mode of operation (only gas phase flowing, $U_{sL} = 0$) or in a continuous mode of operation (both gas and liquid phases flowing).

In spite of all the research efforts, many uncertainties in the design and scale-up of SBC's still exist. In order to design and model an SBC it is necessary to know the axial and radial distributions of solid particles in such a column. Some industrial reactors are known to operate under conditions where not all solids are fluidized (Ellington, 1977). Such reactors do not operate efficiently and it is generally necessary to have complete suspension of solids under normal operating conditions. This requirement generally restricts the solid particle diameters in SBC to less than 2.0×10^{-4} m and makes it necessary for design purposes to have knowledge of critical gas velocity (minimum velocity required to fluidize all solid particles). The available literature on solids behavior in a SBC column can be divided into two parts: (a) critical gas velocity for complete suspension of solids;

Table 1. Solids Distribution Studies

Investigator	SBC Details $D \times 10^{-2}$ m	SBC Details L/m	Mode of Operation	Solid Type (size, μm)	Liquid/Gas (Distributor)	Range of Sup. Velocities 10^2 m/s Liquid	Range of Sup. Velocities 10^2 m/s Gas
Cova (1966)	4.6 6.4 44.7	1.22 1.22 1.22	Continuous	Raney Ni catalyst (15.7)	Water, Acetone/Air (sintered plate)	0.46–6.86	2.59–10.8
Imafuku et al. (1968)	5.0 10.0 20.0	1.0/2.0 1.0/2.0 1.0/2.0	Batch and Continuous	Glass beads ion exchange resin, $FeSiO_2$, Cu (60–180)	Water, Glycerine solution/Air (sieve plate, sintered plate)	0–0.88	2.0–10.0
Farkas and Leblond (1969)	3.8	1.5	Batch	Dowex (126–559)	Water/Air (sieve plate)	0.0	<7.3
Kato et al. (1972)	6.6 12.2 21.4	2.0 1.95 4.06	Batch and Continuous	Glass beads (88–177)	Water/Air (sieve plate)	0.0–2.0	3.6–14.5
Kojima and Asano (1981)	5.5 9.5	1.5 1.5	Batch	Glass beads, acrylic (100, 159 μm)	Water, Glycerol solution/Air (sintered plate)	0.0	1.0–8.0
Brian and Dyer (1984)	12.7 30.5	1.53 4.76	Batch and Continuous	SiO_2, Fe_2O_3 (1–106)	Water, Isoparaffin, Paraffinic oil/Air, N_2 (sieve plate)	0.0–3.0	1.5–16.5
Smith and Ruether (1984)	10.8	1.94	Batch and Continuous	Glass beads (44–210)	Water, EtOH/Air (bubble cap)	2.0	20.0

Table 2. Critical Gas Velocity Investigations

Investigator	SBC Details $D \times 10^{-2}$ m	SBC Details L/m	Mode of Operation	Solid Type (size, μm)	Liquid/Gas (Distributor)	Range of Sup. Velocities 10^2 m/s Liquid	Range of Sup. Velocities 10^2 m/s Gas
Roy et al. (1964)	5.08	1.5	Batch	Quartz, Ni-Alloy, Coal, F-T catalyst (127–675)	Water, Water + Alcohol, Til Oil, Compressor Oil/Air, N_2 (sieve plate)	0.0	N.A.
Narayanan et al. (1969)	11.4 14.1	0.114 0.141	Batch	N.A. N.A.	Water/Air (sieve plate)	0.0	0.5–20.8
Koide et al. (1983)	10.0 14.0 30.0	2.0 2.0 1.9	Batch	Glass beads, brass spheres (78–846)	Water, Glycerol + water, Ethylene glycol + water/Air	0.0	N.A.

and (b) axial and radial solids concentration distributions. The reported studies for (a) and (b) are summarized in Tables 1 and 2, respectively.

Particle behavior in an SBC is influenced by the slip velocity between the solid and liquid phases and by the solids mixing. These, in turn, depend upon (a) solid and liquid phase properties: density, particle size, particle size distribution, viscosity, interfacial tension, and wettability; (b) relative concentrations of solid and liquid phases; and (c) relative velocities of gas and liquid phases.

Previous investigators have described the behavior of solids in an SBC by a one-dimensional sedimentation dispersion model (Cova, 1966; Suganuma and Yamanishi, 1966). Several variations of the model for the steady state conditions have been summarized by Smith and Ruether (1984). The basic assumption made in this model (Cova, 1966) is of uniform particle size, although in most industrial applications the particle size is not uniform. The effect of particle size distribution on hydrodynamic behaviors of an SBC reactor has received very little attention in the literature (Reilly et al., 1982). For polydispersed solids, the solids dispersion coefficient and relative velocity between the solid and liquid phases are dependent on the distribution of particle size and/or density. The sedimentation-dispersion model should therefore be modified to take into consideration the effect of particle size distribution.

In this paper new data for the distributions of monodispersed and polydispersed solids in a semibatch and a continuous SBC are presented. The systems studied are air/nitrogen, water, and a variety of solids. The data are correlated by a modified sedimentation-dispersion model. The model is used to isolate the regions of complete and incomplete fluidization. The effects of liquid and solid properties on the solids distribution are taken into consideration through the empirical correlations for hindered settling velocity and solids dispersion coefficient presented here.

Experimental

Diagrams of the experimental setups used for semibatch and continuous modes of operations are shown in Figures 1 and 2, respectively. Two different columns of 0.0762 m and 0.108 m I.D. were used for batch and continuous runs, respectively. The experimental details of the two columns are given in Table 3 and the physical properties of the solids used in this work are summarized in Table 4.

Axial solids distribution was measured by withdrawing slurry samples from the column through various ports. It was necessary to withdraw a sample from the column as fast as possible in order to have representative data. This was achieved by withdrawing the sample under vacuum and by putting a small diameter tube in the port and withdrawing sample through the tube rather than withdrawing directly through the port.

Both these modifications helped increase the velocity at which the sample was withdrawn, making the sample withdrawal almost instantaneous and thus allowing representative samples for the measurements. The tube also allowed the sampling of solids at various radial positions. The data obtained by this technique were proven to be reproducible by performing duplicate experiments. The concentration of solids in the slurry was determined gravimetrically.

During continuous runs the axial solid concentration distributions were measured under steady state conditions. After steady state conditions were established in the column (experimentally verified as requiring less than one hour of the entire range of

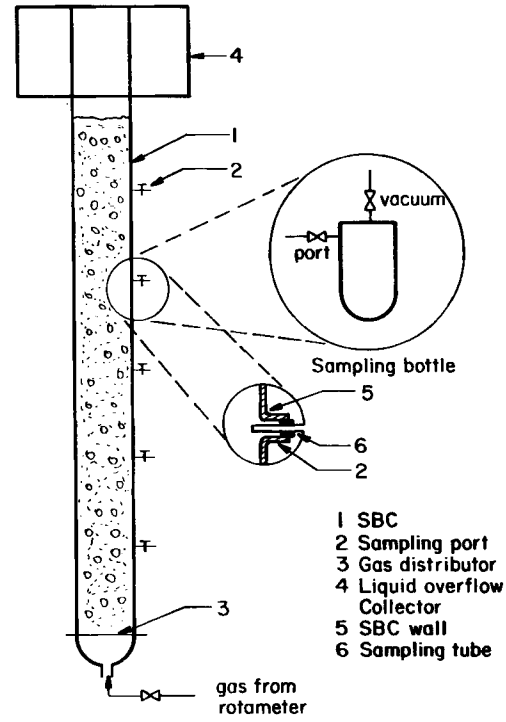

Figure 1. Semibatch slurry bubble column apparatus.

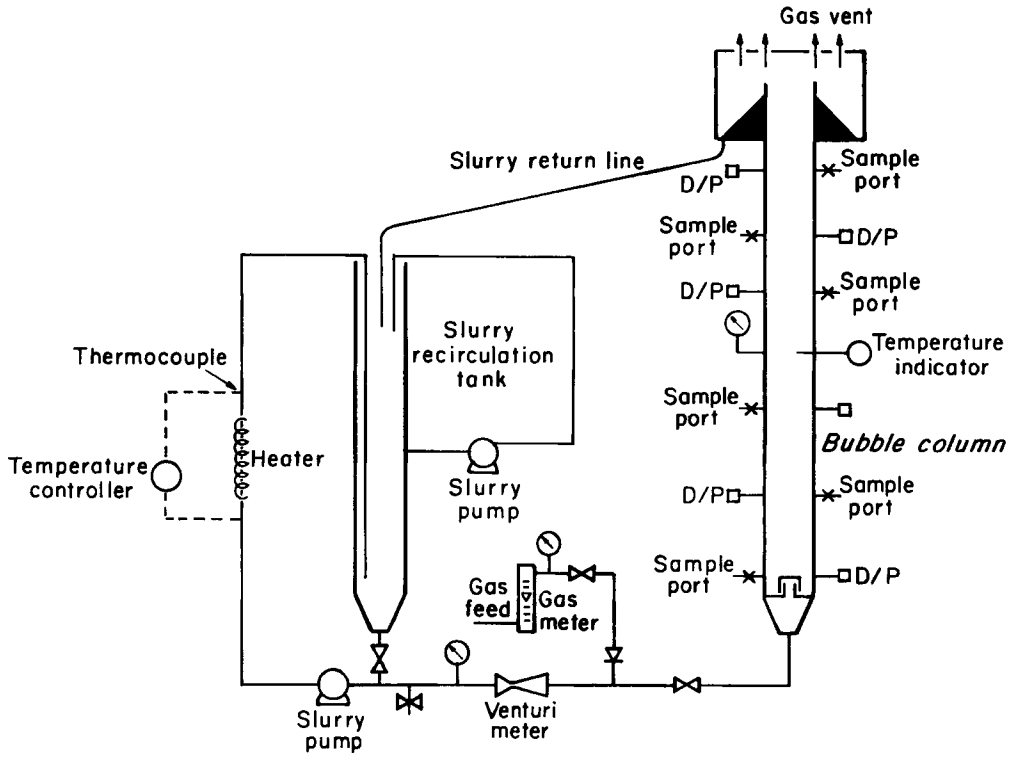

Figure 2. Continuous slurry bubble column apparatus.

experimental conditions), samples of the slurry were withdrawn through sampling ports. All samples were obtained simultaneously with electronically actuated sample valves connected in parallel to a single switch.

The total solids concentration from slurry sampling was obtained gravimetrically. The solids concentration of each narrow-sized fraction in the sample was obtained from pulsed sieve analysis of the dried solids. Gas holdup was calculated from the column height and the settled slurry level in the column after sudden interruption of flows.

Measurements of critical gas velocity

The critical gas velocity (CGV), the minimum superficial gas velocity at which all solids are fluidized, can be determined by visual observations and by pressure drop measurements. However, the opaque nature of slurry and pressure fluctuations may cause inaccuracies in measurements made by these techniques. Bourne and Sharma (1974) and Chapman et al. (1981) presented another technique for measuring CGV in a stirred vessel. They measured the concentration of solids at the bottom of the stirred vessel as a function of gas velocity and found that a discontinuity in this relationship occurs at the CGV. In the present study, the methods of visual observation and Chapman et al. were employed for both glass beads and carborundum particles, and both methods gave similar results in all cases.

Modified Sedimentation-Dispersion Model

For monodispersed particles, the solids concentration distribution in a cocurrent upward flow slurry bubble column operated at steady state conditions appears to be well described by a one-dimensional sedimentation-dispersion model. Smith and Ruether (1984) provide the following mass balance of the solids for the axial position in the column which is a result of solids dispersion, hindered settling, and convection of the solids:

$$-\frac{E_s}{L}\frac{dC_s}{dx}+\left[\frac{\bar{U}_{sL}}{(1-\epsilon_g)}-\bar{\psi}_L U_p\right]C_s = U_{sL}C_s^f \qquad (1)$$

Equation 1 has been derived with the following assumptions: (a) gas holdup is independent of axial position, (b) flow conditions are in steady state, (c) the liquid fraction in the slurry, ψ_L, does not change with axial position, and (d) particle size and density are uniformly constant. Although the liquid fraction in

Table 3. SBC Details

Mode of Operation	Material of Construction	D, Column Dia. m	Column Height m	Gas Distributor	Hole Size m	No. of Holes
Batch	Glass	0.0762	1.54	Sieve plate	0.001	31
Continuous	Acrylic	0.108	1.94	Sieve plate	0.001	72

Table 4. Properties of Solids Used

Solid	Size, D_p μm	Density, ρ_p kg/m^3	Particle Size Distribution
Glass beads	48.5	2,420	No
	46.5	2,420	No
	193.5	2,420	No
Carborundum	84 (avg)	3,870	Yes

the slurry does change slightly with axial position, the value of the average liquid fraction is generally very close to the actual liquid fraction anywhere in the column for a wide range of operating conditions. For the present study, the average liquid fraction was always within 7% of the actual liquid fraction anywhere in the column for the entire range of flow conditions.

For polydispersed particles, a nonuniform particle size establishes nonuniform settling and mixing rates of the solids in the column. The larger particles tend to settle at a higher rate than the smaller particles and to preferentially concentrate near the bottom of the column. In addition to an axial variation in solids concentration, an axial distribution of particle size must also be considered. Separating a distribution of particle size into narrow fractions allows the formulation of a mass balance on each individual narrow fraction of particle size as

$$-\frac{E_{si}}{L}\frac{dC_{si}}{dx}+\left[\frac{\overline{U}_{sL}}{(1-\epsilon_g)}-\bar{\psi}_L U_{pi}\right]C_{si}=U_{sL}C^f_{si} \tag{2}$$

Equation 2 represents a mass balance for the ith particle size fraction in a polydispersed solids system having a solids concentration in the slurry, C_{si}, dependent on the settling and mixing rates of the ith particle characteristics. The hindered settling velocity relative to the column, $\bar{\psi}_L U_{pi}$, takes into account interference of all other particles with the term $\bar{\psi}_L$, the average liquid fraction in the slurry. Integration of Eq. 2 yields an expression in the following form:

$$C_{si}=C_1+C_2\exp\left[-\frac{(\bar{\psi}_L U_{pi}-U_{sL})Lx}{E_{si}}\right] \tag{3}$$

The constants C_1 and C_2 can be determined by consideration of the solids concentration at the bottom and top of the column. Using Eqs. 2 and 3, one can get an expression for C_1 as

$$C_1=-U_{sL}C^f_{si}/(\bar{\psi}_L U_{pi}-U_{sL}) \tag{4}$$

and for C_2 in terms of the solids concentration at the bottom of the column,

$$C_2=C^0_{si}+U_{sL}C^f_s/(\bar{\psi}_L U_{pi}-U_{sL}) \tag{5a}$$

or for C_2 in terms of the solids concentration at the top of the column,

$$C_2=[C^1_{si}+U_{sL}C^f_s/(\bar{\psi}_L U_{pi}-U_{sL})]\exp\left[\frac{(\bar{\psi}_L U_{pi}-U_{sL})L}{E_{si}}\right] \tag{5b}$$

The concentration of solids at the top of the column, C_{si}, may be obtained from a mass balance at $x=1$ in terms of the slurry feed concentration. The concentration gradient at $x=1$ is simply equal to the difference in concentration between the slurry feed concentration and solids concentration at the top of the column. The differential mass balance at the top of the column may be expressed as:

$$-\frac{E_s}{L}\frac{dC^1_{si}}{dx}+U_{sL}C^1_{si}-\bar{\psi}_L U_{pi}C^f_{si}=U_{sL}C^f_{si} \tag{6}$$

where

$$\frac{dC^1_{si}}{dx}=C^f_{si}-C^1_{si}$$

Simplification of Eq. 6 results in the following expression for C^1_{si} in terms of C^f_{si}.

$$C^1_{si}=\left(1+\frac{\bar{\psi}_L U_{pi}}{\dfrac{E_{si}}{L}+U_{sL}}\right)C^f_{si} \tag{7}$$

Combining Eq. 4, 5b, and 7 with Eq. 3 gives the result of the axial solids concentration distribution for the ith particle fraction from the sedimentation-dispersion model as:

$$C_{si}=\left[\left(\frac{E_{si}+\bar{\psi}_L U_{pi}L}{E_{si}+U_{sL}L}\right)\left(\frac{\bar{\psi}_L U_{pi}}{\bar{\psi}_L U_{pi}-U_{sL}}\right)C^f_{si}\right]\cdot\exp\left[-\frac{(\bar{\psi}_L U_{pi}-U_{sL})(x-1)}{E_{si}}\right]-\left(\frac{U_{sL}C^f_{si}}{\bar{\psi}_L U_{pi}-U_{sL}}\right) \tag{8}$$

The total solids concentration in the slurry at any given axial position is the sum of all particle fraction concentrations.

$$C_s=\sum_{i=1}^{n}C_{si} \tag{9}$$

where the solid concentration for the ith particle fraction can be expressed in terms of the sum of all particle fraction as:

$$C_{si}=\phi_i C_s \tag{10}$$

Here ϕ_i is defined as the mass fraction of the ith particle fraction and the following identities are valid.

$$\sum_{i=1}^{n}\phi_i=1 \tag{11}$$

and

$$\sum_{i=1}^{n}\frac{d\phi_i}{dx}=0 \tag{12}$$

Combining Eqs. 9, 10, 11, and 12 with Eq. 2 gives the total solids concentration as a function of axial position

$$\sum_{i=1}^{n}\left(-\frac{E_{si}\phi_i}{L}\right)\frac{dC_s}{dX}+\left[\frac{\overline{U}_{sL}}{(1-\epsilon_G)}-\bar{\psi}_L\sum_{i=1}^{n}(\phi_i U_{pi})\right]C_s=U_{sL}C^f_s \tag{13}$$

The summation term on the lefthand side of Eq. 13 is not constant for polydispersed solids and is a function of axial position. For solids having a greater density than the liquid, the summation term, $\phi_i U_{pi}$, decreases with increasing axial position whereas the summation term, $\phi_i E_{si}$, increases with increasing axial position.

For the analysis of the axial solids concentration distribution,

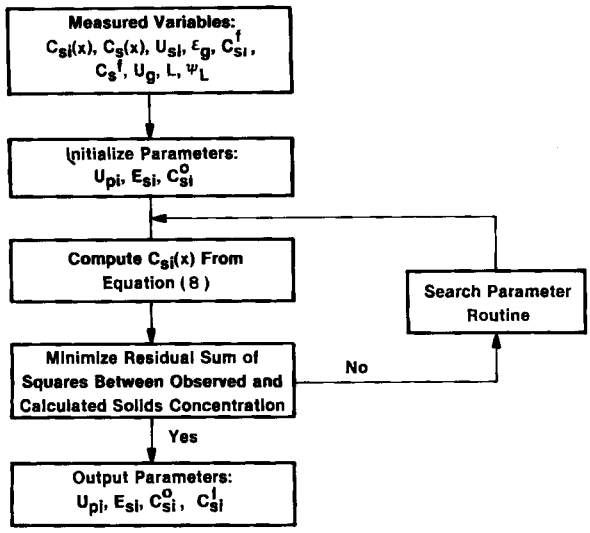

Figure 3. Method of analysis for measured axial solids concentration distributions.

Eq. 8 was used to predict the solids concentration, $C_{si}(x)$, with the best fit of measured solids concentration being optimized with the parameters U_{pi}, E_{si}, and C_{si}^o. For each computation, the six measured slurry concentrations were used and the values of the three parameters were determined to minimize the residual sum of squares between the observed and calculated solids concentration. The objective function employed was

$$F = \sum_{j=1}^{6} [C_{si}(\text{calculated}) - C_{si}(\text{observed})]_j^2 \qquad (14)$$

A search method described by Ahrendts and Baehr (1981) was used to obtain the minimum value of F. The value of F obtained was less than 0.0001 for all experimental conditions. Empirical correlations were then developed for the parameters U_{pi} and E_{si} in terms of the operating variables. The total solids concentration as a function of axial position is then determined from Eq. 8 and the parameter correlations. Figure 3 shows the method of analysis for measured axial solids concentration distributions.

The present model is an improvement on the ones reported earlier by Kato et al. (1972) and Smith and Ruether (1984) in that it does not require the knowledge of C_s^1 or C_s^0. The model also handles a polydispersed system.

For a batch system, putting $U_{sL} = 0$ in Eq. 2 and integrating, the following equation can easily be obtained for a polydispersed system:

$$C_{si} = C_{si}^o \exp\left(-\frac{\psi_L U_{pi} Lx}{E_{si}}\right) \qquad (15)$$

Equations 9 through 12 are also valid in a batch system. Combining Eq. 9–12 and Eq. 15, one can easily obtain the following relationship, which gives the total solids concentration as a function of axial position in a batch system:

$$\sum_{i=1}^{n}\left(\frac{E_{si}\phi_i}{L}\right)\frac{dC_s}{dx} - \left[\psi_L \sum_{i=1}^{n}(\phi_i U_{pi})\right]C_s = 0 \qquad (16)$$

Mapping for Complete and Incomplete Suspension Regimes

The solids concentration distribution as described by the modified sedimentation-dispersion model is valid for completely suspended solids in the slurry. For incomplete suspensions, the solids concentration distribution changes sharply at the interface between suspended and settled solids. The modified sedimentation-dispersion model may be useful for determining the operating conditions for the onset of completely suspended solids or, in other terms, the critical gas/slurry velocity required to completely suspend the solids.

The solids concentration in the slurry for incomplete suspension of solids in a three-phase slurry bubble column has been described mainly in batch slurry operation. For a monodispersed particle size fraction, the solids concentration distribution for a batch system may be obtained from integration of Eq. 1 with $U_{sL} = 0$.

$$C_s = C_s^0 \exp(-\bar{\psi}_L U_p Lx/E_s) \qquad (17)$$

Integration of Eq. 17 yields the average solids concentration in terms of the solids concentration at the bottom of the column.

$$\bar{C}_s = \frac{C_s^0}{A}[\exp(A) - 1] \qquad (18)$$

where

$$A = -\bar{\psi}_L U_p L/E_s$$

Under conditions where the solids are not completely suspended in the bubble column, the solids at the bottom of the column will be stationary and have a greater concentration than the suspended solids concentration. The concentration of settled solids in slurry is related to the packing density of settled solids. The void fraction of solids at minimum fluidization conditions can be used to estimate the packing density. Matheson et al. (1949) give the following expression for packing density of solids in a two-phase system for particles smaller than 500 microns and larger than 50 microns.

$$\epsilon_S^M = 0.155 \ln D_p + 1.78 \qquad (19)$$

The concentration of settled solids in slurry is related to the void fraction of solids by the following expression.

$$C_S^M = \frac{\epsilon_S^M \rho_S}{(1 - \epsilon_g)} \qquad (20)$$

For the onset of incomplete suspension of solids, the solids concentration in the settled slurry may be related to the concentration of solids just above the settled slurry.

$$-\frac{E_S}{L}\frac{dC_S^M}{dx} - \bar{\psi}_L U_p C_S^0 = 0 \qquad (21)$$

The solids concentration gradient, dC_S^M/dx, is defined as $C_S^0 - C_S^M$. Combining Eqs. 21 and 17 and rearranging, the following expression is derived for the onset of incomplete suspension of

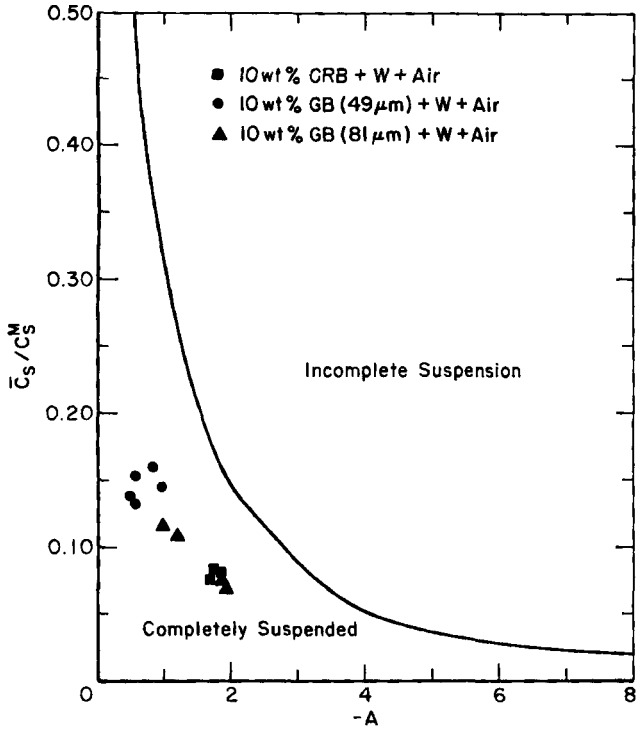

Figure 4. Mapping of complete and incomplete solids suspension.

solids:

$$C_S^M = (1 - A)\, C_S^0 \tag{22}$$

Combining Eqs. 22 and 18 yields the following expression:

$$\frac{\bar{C}_S}{C_S^M} = \frac{(\exp A - 1)}{(1 - A)A} \tag{23}$$

Thus, a criterion for incomplete suspension of solids is given by combining Eqs. 19, 20, and 23. For completely suspended solids, the following inequality must be satisfied:

$$\bar{C}_S < \frac{(0.155 \ln D_p + 1.78)\, \rho_s\, (\exp A - 1)}{(1 - \epsilon_g)\, (1 - A)A} \tag{24}$$

The inequality in Eq. 24 is presented in Figure 4 as a mapping separating the regions of complete and incomplete fluidization.

Results and Discussion

Gas holdup

Average gas holdup data obtained in a slurry bubble column were compared with several correlations in the literature (Akita and Yoshida, 1973; Hikita et al., 1980; Hughmark, 1967). The best agreement between observed and predicted gas holdup for the water system was obtained with the correlation proposed by Hughmark, as given by the following expression:

$$\epsilon_g = [2 + (0.35/\bar{U}_g)\, (\rho_L \sigma/72)^{1/3}]^{-1} \tag{25}$$

The maximum deviation between observed and predicted gas holdup was less than 15% with an average deviation of 6.7%. The range of gas holdup and superficial gas velocity was from 0.095 to 0.285 and from 0.031 to 0.20 m/s, respectively. Liquid surface tension and density remained essentially constant at 0.072 N/m and 1,000 kg/m^3, respectively.

Hindered settling velocity

The hindered settling velocity, U_p, for a slurry bubble column represents the slip velocity between the solid and liquid phases. The hindered settling velocities obtained in this investigation by the method shown in Figure 3 are predicted well with the correlations given by Kato et al. (1972) and Smith and Ruether (1984). These correlations predict a dependency of the hindered settling velocity on the terminal particle velocity, gas velocity, and average liquid holdup in the slurry. Since the average liquid holdup in the slurry was not varied significantly in the present investigation ($0.942 < \bar{\psi}_L < 0.965$), the dependency of hindered settling velocity on this variable is assumed to be the same as given by Smith and Ruether. A regression analysis of the hindered settling velocity on operating variables has given the following equation:

$$U_p = 1.44\, U_t^{0.78}\, \bar{U}_g^{0.23}\, \bar{\psi}_L^{3.5} \tag{26}$$

The average absolute relative deviation between the observed hindered settling velocity and that predicted from Eq. 26 is 9.6%. The range of terminal particle velocities is from 0.002 to 0.022 m/s. Figure 5 shows the effect of gas velocity on the hindered settling velocity. Equation 26 applies to each narrow-sized

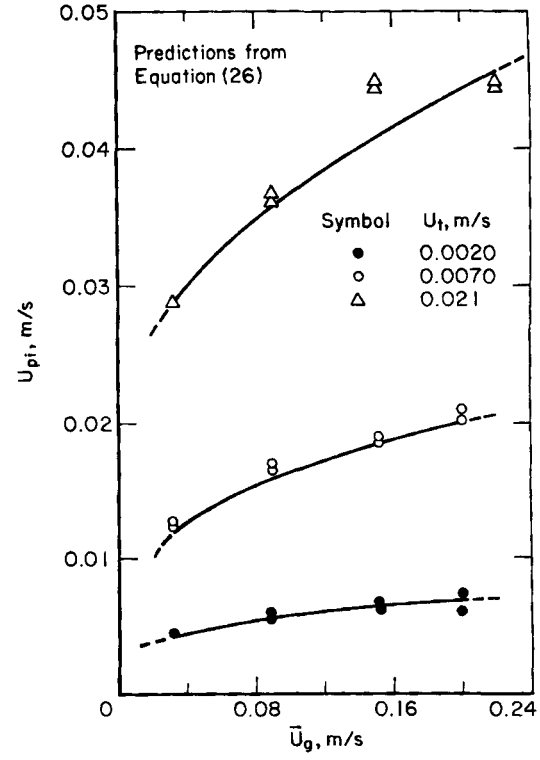

Figure 5. Effect of gas velocity on hindered settling velocity.

fraction of solids in the slurry bubble column having a unique terminal particle velocity. The terminal particle velocity may be obtained from an analytical expression provided by Zigrang and Sylvester (1981). From this correlation, it is evident that for polydispersed solid systems the hindered settling velocity is little affected by particle-particle interaction and that the particles behave as well-dispersed solids.

Solids dispersion coefficient

A dimensionless analysis of the solids dispersion coefficient in terms of a solids Peclet number, similar to the expression given by Smith and Ruether, has been used to correlate the dependence of the solids dispersion coefficient on operating variables. A regression analysis of the experimental data yields the following expression:

$$Pe_p = 6.7\ (Fr_g^6/Re_g)^{0.106}\ (1 + 0.15\ Re_p) \qquad (27)$$

The above relation is valid on the ranges of $0.25 < Pe_p < 1.3$; $300 < Re_g < 2{,}700$; $0.03 < Fr_g < 0.20$; and $0.1 < Re_p < 5$. In the case of continuous operation, greater than 90% of solids Peclet numbers were predicted within ±20% of observed values.

Critical gas velocity (CGV)

The CGV mapping discussed earlier was used to predict the regime of operation of the slurry bubble column. The coordinates of the CGV mapping presented in Figure 4 were estimated by using the correlations and equations presented earlier for glass beads of all sizes and carborundum particles. All experiments of solids distribution performed above were visually observed CGV and all points for the above-mentioned solids should be in the completely suspended region. As can be observed in Figure 4, the mapping works well for all solids.

Concentration distribution of solid particles in batch and continuous operations

The experimental solids distribution data obtained in batch operation for three different sizes of glass beads and their mixture are presented in Figures 6 through 9 for two different superficial gas velocities. As can be seen in Figure 9, the concentration profile of the mixture of glass beads is completely different from that obtained for glass beads of 81 μm size, even though this size is closer to the average particle size of the mixture. It can also be observed in these figures that the distribution of glass beads is only slightly affected by the increase in superficial gas velocity from 6.7 to 11.0 cm/s. This can be explained by the present data, which show that both axial dispersion coefficient and hindered settling velocity increase with gas velocity. The ratio U_p/E_s, which determines axial solid distribution, changes little with gas velocity.

The concentration profiles predicted by the correlations for U_p and E_s by Kato et al. (1972) and those obtained by the analysis of data using the model and correlations proposed in this work are also shown in Figures 6 through 8. As can be observed in Figures 6 and 7, very little difference exists between the concentration profiles predicted by these two correlations in the case of monodispersed solids. However, as can be seen in Figure 8, the model for polydispersed solids predicts a concentration profile that is in very good agreement with the experimental data as compared to that predicted by the correlation proposed

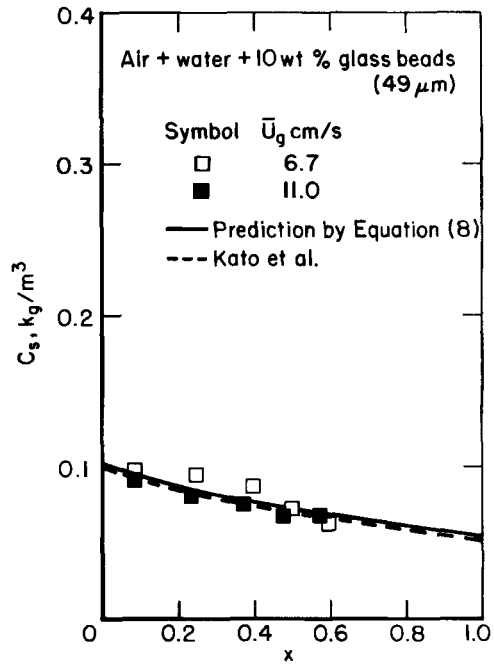

Figure 6. Axial solids concentration distribution for 49 μm particles (semibatch operation).

by Kato et al. using an average size of glass beads. A comparison of axial solids concentration distributions for monodispersed and polydispersed particles is given in Figure 9.

The experimental solids distribution data obtained in a continuous system for three different sizes of glass beads and their mixture are presented in Figure 10 for continuous operation. As can be seen from this figure, the concentration distribution of a

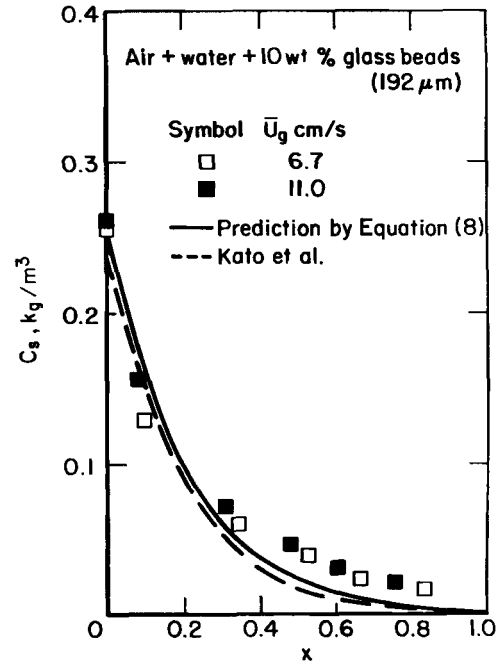

Figure 7. Axial solids concentration distribution for 192 μm particles (semibatch operation).

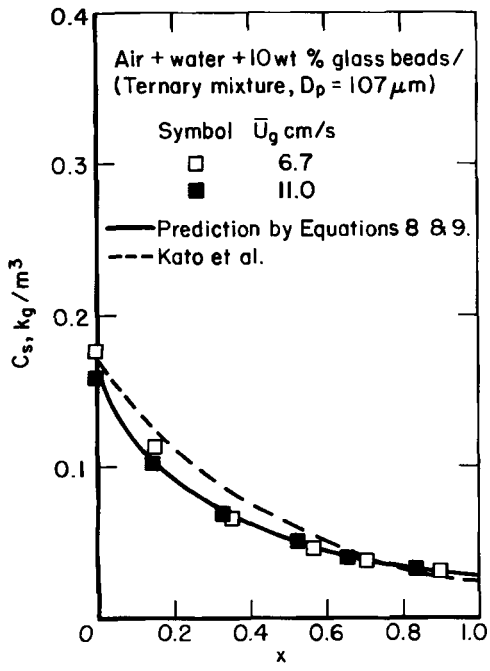

Figure 8. Axial solids concentration distribution for ternary mixture of narrow-sized particles (semibatch operation).

mixture of glass beads shows a completely different trend as compared to monodispersed solids under identical conditions. It can be observed from the figure that the model presented in this work predicts the concentration distribution of polydispersed solids in continuous modes of operation reasonably well. The effect of slurry velocity on the solids concentration distribution

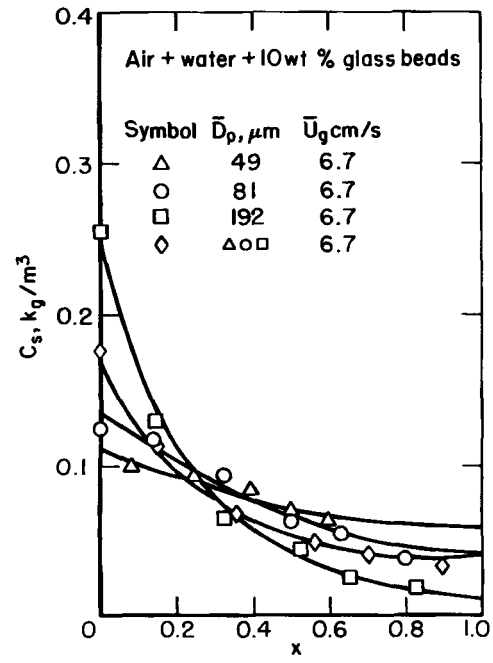

Figure 9. Comparison of axial solids concentration distributions for monodispersed and polydispersed particles (semibatch operation).

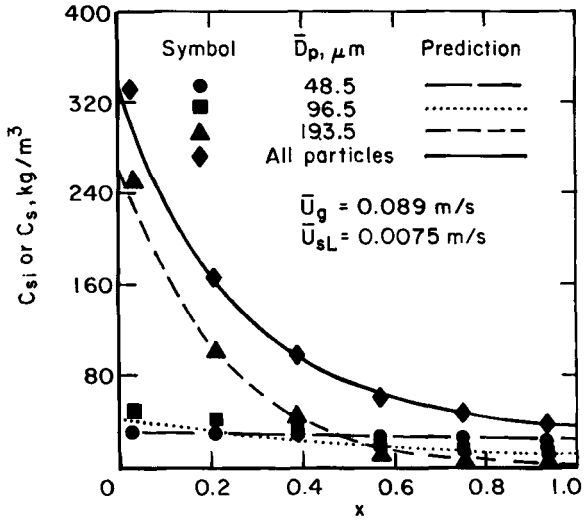

Figure 10. Axial solids concentration distribution for ternary mixture of narrow-sized particles (continuous operation).

is illustrated in Figure 11. Once again, as shown, the present model predicts the results reasonably well for all operating conditions.

The change in average particle diameter with axial position for a ternary mixture of solids is shown in Figure 12. The large variation in average particle size is attributed to the segregation effect caused largely by the differences in hindered settling velocities of the ternary mixture. As can be seen, the particle size as a function of axial position can be well predicted from the present modified sedimentation-dispersion model.

The mean particle size for polydispersed solids is calculated from the following expression

$$\bar{D}_p = \sum_i^n \phi_i D_{pi}$$

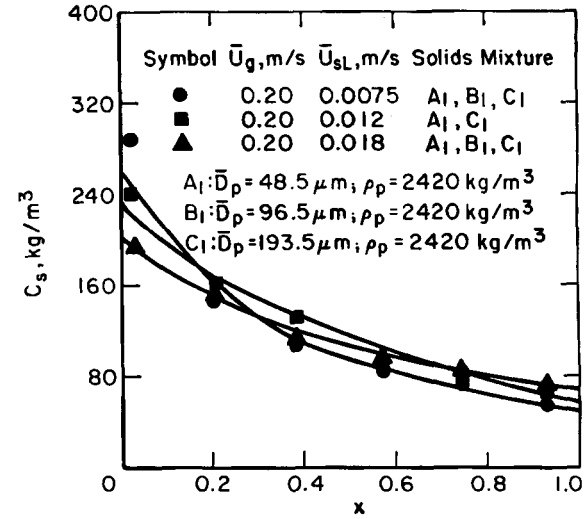

Figure 11. Effect of slurry velocity on axial solids concentration distribution.

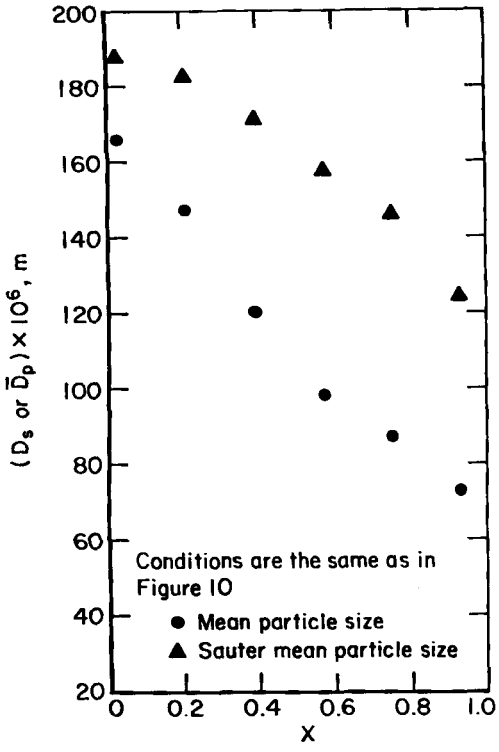

Figure 12. Axial mean particle size distribution for ternary mixture of glass beads.

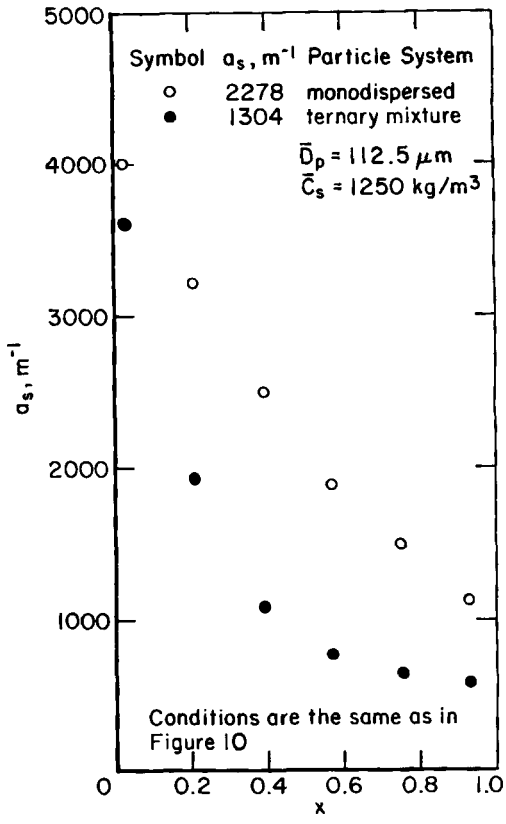

Figure 13. Comparison of axial specific surface area distribution for monodispersed and polydispersed particles having the same mean particle size and average solids concentration.

Another important aspect in characterization of the solids is the distribution of the Sauter mean particle size, which may be calculated as follows:

$$D_s = \sum_i^n \phi_i D_{pi}^3 / D_{pi}^2$$

The Sauter mean particle size can be used directly in the calculation of the specific interfacial area of solids:

$$a_s = 6\,(1 - \epsilon_g)\, C_s / \rho_s D_s$$

For polydispersed solids, the larger particles concentrate near the bottom of the column where the solids concentration is the greatest and it was postulated that this would minimize the axial specific interfacial area. However, a comparison of the specific interfacial area for monodispersed and polydispersed particle systems is given in Figure 13, and the axial variation of the interfacial area for the polydispersed system is larger than for the monodispersed system. In addition, the average solids interfacial area is greater for the monodispersed solids than for the polydispersed particles. This is typical for all solid systems used in this study. Therefore, operation with a particle distribution as narrow-sized as possible will minimize mass transfer resistance of the solids.

Notation

A = parameter in Figure 5 $= -(\bar{\psi}_L U_p L / E_s)$
a_s = specific interfacial area of solids, m^{-1}
C_s = concentration of solids in slurry sample withdrawn, kg/m³ of slurry
C_s^1 = concentration of solids at top of column, kg/m³ of slurry
$\bar{C}_s$ = average solids concentration in slurry column, kg/m³ of slurry
C_s^0 = concentration of solids at bottom of column, kg/m³ of slurry
C_s^m = concentration of solids in settled solids, kg/m³ of slurry
C_s^f = concentration of solids in slurry feed, kg/m³ of slurry
C_{si} = concentration of solids for its particle size fraction, kg/m³ of slurry
C_μ = viscosity correction factor = $1.5/89{*}10^{-1} \log \mu_L + 1.026 \times 10^{-1} \log^2 \mu_L$ for μ_L in cp
C_1, C_2 = constants defined in Eq. 3
D = diameter of column, m
D_d = diameter of distributor, m
D_p = diameter of particle, m
D_s = Sauter mean particle diameter, m
$\bar{D}_p$ = weight average diameter of particle, m
E_L = longitudinal dispersion coefficient for liquid, m²/s
E_s = longitudinal dispersion coefficient for solid, m²/s
Fr_g = Froude number $= U_g / \sqrt{gD}$
g = gravitational acceleration, m/s²
L = dispersion height of slurry, m
L_o = height of the unaerated liquid column, m
Pe_p = Peclet number based on $Es = \bar{U}_g D / E_s$
Re_T = gas Reynolds number $\bar{U}_g D \epsilon_G / \mu_g$
Re_g = Reynolds number based on column diameter $= \bar{U}_g D \rho_L / \mu_L$
Re_p = Reynolds number based on particle diameter $= \bar{U}_g D_p \rho_L / \mu_L$
$\bar{U}_g$ = superficial gas velocity, m/s
U_{sL} = linear liquid velocity, m/s
$\bar{U}_{SL}$ = superficial liquid velocity, m/s
U_p = settling velocity of solid particles in aerated column, m/s
U_t = terminal settling velocity of a single particle in stagnant liquid, m/s
$x = z/L$ normalized axial height from the distributor plate
z = axial distance from the distributor plate

Greek letters

ϵ = gas phase holdup
π = density, kg/m^3
σ = surface tension, n · m^{-1}
μ = viscosity, kg/m · s
ψ_L = volume fraction of liquid in slurry = 1 − (volume fraction of solid particle in slurry)
$\bar{\psi}_L$ = average volume fraction of liquid in slurry
ϕ = weight fraction of narrow-sized particles

Subscripts

g = gas
i = ith particle size
ρ, L = liquid
s, p = particle/solid

Superscripts

f = slurry feed

Literature Cited

Ahrendts, J., and Ito Baehr, "The Use of Nonlinear Regression Analysis in Establishing Thermodynamic Equations of State," *Int. Chem. Eng.*, **21**, 572 (1981).

Akita, K., and G. Yoshida, "Gas Holdup and Volumetric Mass Transfer Coefficient in Bubble Columns," *Ind. Eng. Chem. Proc. Des. Dev.*, **12**, 76 (1973).

Bourne, J. R., and R. N. Sharma, Proc. 1st European Conf. on Mixing, B325, BHRA Cranfield (1974).

Brain, B. W., and P. N. Dyer, "The Effect of Gas and Liquid Velocities and Solid Size on Solid Suspension in a Three-Phase Bubble Column Reactor," *Chemical and Catalytic Reactor Modeling*, M. P. Dudukovic, and P. L. Mill, eds., ACS Symp. Ser. **237**, 107 (1984).

Chaudhary, R. V., and R. A. Ramachandran, "Three-Phase Slurry Reactors," *AIChE J.*, **26**, 177 (1980).

Chapman, C. M., A. W. Nienow, and J. C. Middleton, "Particle Suspension in a Gas Sparged Rushton-Turbine Agitated Vessel," *Trans. Inst. Chem.* **59**, 134 (1981).

Cova, D. R., "Catalyst Suspension in Gas-Agitated Tubular Reactors," *Ind. Eng. Chem. Proc. Des. Dev.*, **5**, 20 (1966).

Ellington, R. T., *Liquid Fuels from Coal*, Academic Press, New York, 90 (1977).

Farkas, E. J., and P. F. Leblond, "Solid Concentration Profile in the Bubble Column Slurry Reactor," *Can. J. Chem. Eng.*, **47**, 215 (1969).

Hikita, H., et al., "Gas Holdup in Bubble Columns," *Chem. Eng. J.*, **20**, 59 (1980).

Hughmark, G. A., "Holdup and Mass Transfer in Bubble Columns," *Ind. Eng. Chem., Proc. Des. Dev.*, **6**, 218 (1967).

Imafuku, K., et al., "The Behavior of Suspended Solid Particles in the Bubble Column," *J. Chem. Eng. Japan*, **1**, 153, (1968).

Kato, Y., et al., "The Behavior of Suspended Solid Particles and Liquid in Bubble Columns," *J. Chem. Eng. Japan*, **5**, 112 (1972).

Koide, K., et al., "Critical Gas Velocity Required for Complete Suspension of Solid Particles in Multistage Bubble Columns," *J. Chem. Eng. Japan*, **17**, 7 (1983).

Kojima, H., and K. Asano, "Hydrodynamic Characteristics of a Suspension Bubble Column," *Int. Chem. Eng.*, **21**, 473 (1981).

L'Homme, G. A., "Introduction to the Applied Physical Chemistry and Chemical Engineering Problems Set by Gas-Liquid-Solid Catalyst Reactions and Reactors," *Chemical Engineering of Gas-Liquid-Solid Catalyst Reactions*, G. A. L'Homme, ed., CEBEDOC/Liege (1979).

Matheson, G. L., W. A. Herbst, and P. A. Holt, "Characteristics of Fluid-Solid Systems," *Ind. Eng. Chem.*, **41**, 1,099 (1949).

Narayanan, S., V. K. Bhatia, and D. K. Guha, "Suspension of Solids by Bubble Agitation," *Can. J. Chem. Eng.*, **47**, 360 (1969).

Reilly, I. G., D. S. Scott, and M. Abou-El-Hassau, "Leaching in a Bubble Column Slurry Reactor," *Can. J. Chem. Eng.*, **60**, 399 (1982).

Roy, N. K., D. K. Guha, and M. N. Rao, "Suspensions of Solids in a Bubbling Liquid," *Chem. Eng. Sci.*, **19**, 215 (1964).

Smith, D. N., and J. A. Ruether, "Dispersed Solid Dynamics in a Slurry Bubble Column," *Chem. Eng. Sci.*, **4**(5), 741 (1985).

Suganuma, T., and T. Yamanishi, "Concentration Gradient in Multiple Stage Gas Bubble Columns," *Kagaku Kogaku Ronbunshu*, **30**, 1,136 (1966).

Zigrang, D. J., and N. D. Sylvester, "An Explicit Equation for Particle Settling Velocities in Solid-Liquid Systems," *AIChE J.*, **27**, 1,043 (1981).

Manuscript received Nov. 13, 1984, and revision received Apr. 23, 1985.